Journal of Engineering Sciences and Information Technology
Volume (6), Issue (5): 30 Sep 2022
P: 81 - 98

ISSN: 2522-3321

مجلة العلوم الهندسية وتكنولوجيا المعلومات
المجلد (6)، العدد (5): 30 سبتمبر 2022م
ص: 81 - 98

Influence of Bentonite Nanoparticles on properties of PVP-CMC-Gums Hydrogel Films for biomedical applications

Samahir Abdalla Sheikh Idris

Ozgun Yucel

Engineering College || Gebze Technical University || Turkey

Abstract: Recently, polymers have been widely employed, and the unique features of hydrogels have found several applications, particularly in biomedical applications. In this work, PVP-CMC-Gums hydrogel films were created from a variety of materials using casting and room-temperature drying processes; however, the impacts of adding bentonite clay, SEM, FTIR, XRD, TGA, swelling, melting, contact angle, and a set of experiments were performed to clarify and analyze a variety of physical, mechanical, thermal, and other characterizations. The main results revealed new peaks indicative of the presence of cross-linking, which is a major driver of loading and release properties, suggesting that these films can be used for drug delivery and a variety of other applications. PCXB film has the best properties in color, surface hydrophobicity, solubility, and swelling, while PCGB film has the best results in biodegradability and permeability, and the two films have strong thermal, and mechanical and release properties. Accordingly, the addition of bentonite clay to hydrogel films improves all their properties, making them suitable for diverse biomedical applications such as root canal fillings, tissue engineering, contact lenses, and dressings.

Keywords: Hydrogel, cross-linking, Biomedical application, Bentonite, Gums.

تأثير جسيمات البينتونيت النانوية على خصائص أفلام الهيدروجيل PVP-CMC-Gums للتطبيقات الطبية الحيوية

سماهر عبد الله شيخ إدريس

اوزقون يوجيل

كلية الهندسة || جامعة جبزى التقنية || تركيا

المستخلص: تُستخدم البوليمرات في الآونة الأخيرة على نطاق واسع، والخصائص العديدة للهيدروجيل تدخل استخدامات شتى، لاسيّما في التطبيقات الطبية الحيوية. صُنعت أفلام الهيدروجيل PVP-CMC- Gums من مجموعة متنوعة من المواد بواسطة تقنيات الصب والتجفيف تحت درجة حرارة الغرفة في هذه الورقة، دعت الحاجة إلى دراسة تأثيرات إضافة طين البنتونيت، واستُخدم كلا منSEM و FTIR و XRD و TGA والتورم والذوبان وزاوية التلامس ومجموعة من الدراسات الأخرى لتوضيح وتحليل مجموعة متنوعة من الخصائص الفيزيائية والميكانيكية والحرارية وغيرها. كشفت النتائج الرئيسية قِمَمًا جديدة، تشير إلى إنشاء روابط متقاطعة، وهي تُعد سببًا رئيسيًا في خصائص التحميل والإطلاق، ممَّا يشير إلى أنه يمكن استخدام هذه الأفلام في توصيل الأدوية ومجموعة مختلفة من التطبيقات الأخرى. يمتاز فيلم PCXB بأفضل خصائص في اللون، ومقاومة الماء للسطح، والقابلية للذوبان، والتورم، بينما يمتاز فيلم PCGB بأفضل نتائج في قابلية التحلل البيولوجي والنفاذية، والفلمان لهما خصائص حرارية وميكانيكية وإطلاق قوية. وفقا لذلك، فإن إضافة طين البنتونيت إلى

أغشية الهيدروجيل يحسن جميع خصائصها، مِمَّا يجعلها مناسبة لمجموعة متباينة من التطبيقات الطبية الحيوية مثل حشوات جذور الأسنان، وهندسة الأنسجة، والعدسات اللاصقة، والضمادات.

الكلمات المفتاحية: هيدروجيل، الربط المتقاطع، التطبيقات الطبية الحيوية، البنتونيت، اللثة.

1- INTRODUCTION.

Biomaterials have a massive effect on human health care. They are vastly used in biomedical applications because of their biocompatibility, biodegradability, non-toxicity, good structural properties, thermal abilities, and good broad characterizations. One of these biomaterials is hydrogel (Gils, et al., 2009, p.364). Hydrogel knows as a water-swollen polymer with a three-dimensional structure or crosslinking; it can absorb and retain aqueous solutions up to a hundred times its weight; it is also characterized by hydrophilicity and insolubility in water (Ma, et al., 2015)- (Ray, et al., 2010, P.1703). All the properties of hydrogels have been considered essential in many ways, where they can be used for various pharmaceutical and biomedical applications, such as drug delivery and tissue engineering, tooth root fillings, contact lenses, bandages, and more (Gils, et al., 2009, p.364).

Gums-based hydrogels have created extensive interest as biomaterials (Gils, et al., 2009, p.364). Hydrogel is considered a cheap, effective, and convenient material for bio applications (Ray, et al., 2010, p.130). Also, it is used in other applications such as packaging materials (Bandyopadhyay, et al., 2010), (Bandyopadhyay, et al., 2020, p.307). Polyvinylpyrrolidone (PVP) is a polymer that soluble in water and made from the monomer N-vinylpyrrolidone (Haaf, et al., 1985, p.143). It has unique features which make it one of the best polymers that can be used with the human body, such as colloid protection, viscosity, hygroscopicity, hydrotropic, coagulation, high physiological adaptability, strong bonding ability (Hsiao & Huang, 2005, p.1936); PVP polymer can be used as one of the main components of the hydrogel preparation. PVP hydrogel itself does not display good swelling features, but when mingled with polysaccharides such as carboxymethylcellulose (CMC), their swelling properties upgrade (Ray, et al., 2010, p.130). CMC is involved in semisynthetic polymers, the most abundant organic material in nature (Batelaan, et al., 1992, p.329); CMC has many properties, especially biocompatibility, biodegradability, non-toxicity, cost-effectiveness, good physicochemical properties (Kanikireddy, et al., 2020, p.963). Agar (AG) acts as a natural cross-linking agent, and its gelling characteristics provide mechanical reinforcement in hydrogels (Ray, et al., 2010, p.130). Agar has various properties; no need to add reagents to generate gelation; it is used among a wide range of pH, and is very stable, not causing a residue (Armisen & Galatas, 1987, p.1). Polyethylene glycols (PEGs) are hydrophilic polymers; It has many properties such as being non-toxic, colorless, inert, odorless, non-volatile, soluble in water, and organic solvents, it is retaining moisture and has excellent absorbing and binding features. Also, its thermal stability is desired for various biomedical applications, PEG with crosslinking agents such as PVP, a strengthening agent, provides an impetus to the hydrogel's gelling behaviour (Hutanu, et al., 2014, p.1). Guar gum (GG) is obtained from

guar beans. Its source is an annual pod-bearing called Guar. It has good additive properties; it emulsifies, binds water, inhibits ice crystals in frozen products, moisturizes, thickens, stabilizes, binding by hydrogen bond formation and gelling properties apart from easy solubility in cold water, wide pH tolerance, high thermal stability film-forming ability and biodegradability and suspends many liquid-solid systems (Bandyopadhyay, et al., 2019), (Mudgil, et al., 2014, p.409). Xanthan gum (XG) is an extracellular polysaccharide secreted by the microorganism Xanthomonas campestris. XG offers a potential utility as a drug carrier because of its inertness and biocompatibility. Also, Xanthan solutions are highly viscous even at low polymer concentrations (Gils, et al., 2009, p.364), (Garcıa-Ochoa, et al., 2000, p.549). Geologists define Bentonite (BE) as a rock formed of highly colloidal and plastic clays composed mainly of montmorillonite. The unique characteristics of bentonite are the ability to form thixotropic gels with water and absorb vast quantities of water with an accompanying increase in the volume of 12–15 times its dry bulk and a high cation exchange capacity (Adamis, et al., 2005). The clay application is usually in the form of a powder, suspension, emulsion, or gel (Stojiljković & Stojiljković, 2017, p.349).

Rare reports were available on the synthesis of hydrogels made from GG and XG, but no substantial work has been reported to grafting BE onto XG and GG hydrogels. The present article is based on the synthesis and characterization of crosslinking hydrogel by grafting BE onto XG and GG hydrogels and its abilities to be used in different biomedical applications. So, the characterizations of the films were studied based on the changes that happened based on the gums additions and gums with Be additions.

2- MATERIAL AND METHODS.

2-1 Material:

The polyvinylpyrrolidone (PVP), Guar gum (GG), and Xanthan gum (XG) were procured from Sigma Aldrich, USA. The carboxymethyl cellulose (CMC) was procured from Sinopharm Chemical Reagents Co. Ltd. Polyethylene glycol (PEG) and agar (AG) were supplied by Fluka, CZ. Glycerine (Gly) was obtained from LachNer, CZ. Bentonite (BE) was purchased from Shanghai No.4 Reagent & H.V. Chemical Co., Ltd.

2-2 Methods:

2-2-1 Production of Hydrogel based PVP-CMC-GG (PCG), PVP-CMC-XG (PCX), PVP-CMC-GG-BE (PCGB), and PVP-CMC-XG-BE (PCXB) films:

The hydrogel films were produced by casting method in laboratory Petri dishes; the composition of the films is mentioned in Table 1. Then all the components were mixed in a magnetic stirrer at 500 rpm for 30 min. Then the mixtures were put in an ultrasonic device for 15 min. After that, the mixture was exposed to heat for 45 min in an autoclave at 121 °C. Finally, the mixtures were poured into the dishes

using a transfer pipet. All the dishes were left at room temperature (23-25) °C to dry for two days. Later they were peeled off from the trays using the tweezers (Bandyopadhyay, et al., 2010).

Table (1) The compositions of the Hydrogel films.

Hydrogel films	PVP (g)	CMC (g)	AG (g)	PEG (ml)	GLY (ml)	GG (g)	XG (g)	BE (g)	H_2O (ml)
PCG	1	0.5	3	1.5	1.5	0.4	-	-	150
PCX	1	0.5	3	1.5	1.5	-	0.4	-	150
PCGB	1	0.5	3	1.5	1.5	0.4	-	0.7	150
PCXB	1	0.5	3	1.5	1.5	-	0.4	0.7	150

2-2-2 Light Microscope Analysis:

The surface structures of the films were studied under the Compound Light Microscope from (SOIF XDS-1B, USA), all the images were captured at a magnification of 50x.

2-2-3 Scanning Electron Microscope:

The films' cross-sectional and surfaces morphologies were studied under a field emission scanning electron microscope (Nova NanoSEM™ by FEI™, USA); the films were dried and sputter-coated with a thin layer of gold for better surface conductivity for 60 s at 30 mA. (Bandyopadhyay, et al., 2019) The images were captured at a magnification of 250- 5000x and 2 kV, 5 kV, and 10 kV.

2-2-4 Fourier-Transformed Infrared Spectroscopy:

The functional group analysis of the samples was done using Fourier transfer infrared (FTIR) spectroscopy in an attenuated total reflectance (ATR) mode (Nicolet iS5 by Thermo Scientific, USA) (Bandyopadhyay, et al., 2020, p.307). The results are reported from a scanning range of 4000 to 500 cm^{-1} with an average of 16 scans and a resolution of 4 cm^{-1}.

2-2-5 X-Ray Diffraction:

XRD technique was applied to know the crystalline structure of the films; the tests were done using an x-ray diffractometer (MiniFlex™600 x-ray diffractometer, Rigaku, Japan). The divergence slit was maintained at 0.1° throughout the experiment. The scans were executed in the range of 4°—70° at a speed of 5° min^{-1} utilizing a foil filtered Co Kβ radiation (λ of 0.179 nm) at 40 kV and a current of 15 mA (Bandyopadhyay, et al., 2010).

2-2-6 Tensile Analysis:

The tensile strength analysis was analyzed using the dynamometer Instron 5567 (Instron, USA). The samples for mechanical tests were cut in the dimension of 80mm in length x 15mm wide. An average

thickness of 0.13 ± 0.05, with a static load of 5 kg and a crosshead speed of 10 mm min^{-1}, at room temperature 24 °C (Bandyopadhyay, et al., 2010), all the data represent an average of eight replications.

2-2-7 Colour Analysis:

The determination of color is essential for selecting the best films for specific biomedical applications based on color. The color was determined using NR100 Precision Colorimeter (Bandyopadhyay, et al., 2010). The L, a, and b values were obtained using the CIE lab scale. The total color difference (ΔE) and Chroma (C) were calculated with the following equations:

$$\Delta E = \sqrt{(\Delta L)^2 + (\Delta a)^2 + (\Delta b)^2} \quad (2.1)$$

$$\Delta L = L - L0 \quad (2.2)$$

$$\Delta a = a - a0 \quad (2.3)$$

$$\Delta b = b - b0 \quad (2.4)$$

$$C = (a)2 + (b)2 \quad (2.5)$$

The standard values for L, a, and b are 93.02,-0.46, and 3.58, respectively, and L0, a0, and b0 are the color parameters of each film.

2.2.8 Contact angle analysis:

The best explanation of contact angle is the "angle between a liquid and a solid within the body of the liquid formed at the gas-liquid-solid interface," the contact angle was determined through a static contact angle measuring System (Advex Instruments s.r.o, CZ) at RT 23 °C and RH 57% (Bandyopadhyay, et al., 2019). The films' dimension was 15 mm in length and 40 in mm width; images of both (lower and upper) surfaces of the films were captured after 5µl of water was dropped on the film surface using a micropipette. All the data represent an average of five replications for every side.

2.2.9 Water vapor permeability:

By using (cup method) water vapor permeability (WVP) was measured. An easy explanation of WVP is the moisture that penetrates the film. The cup has a circular radius of 20 mm, and the test area is 140.56 mm^2. The films are bigger than the cup radius, which covers an area of around 150 mm^2. The films were put and sealed to the cups with special silicone gel which is highly resistant to the passage of water vapor. Inside the cup, silica beads were put with a known amount. The empty cup, the cup with silica, and the cup with the film and silica were weighted. All the cups were kept inside a climate desiccator at 20 °C and 90 ± 2 % RH for 24 hr. The final measurement was done after 24 hr of incubation in the climate chamber (Bandyopadhyay, et al., 2019). The WVP was calculated using the following equations:

$$WVP = (WVTR \times \delta)/\Delta P \qquad (2.6)$$

where WVTR is the measured water vapor transmission rate through the film,

$$WVTR = \Delta W/ (A \times t) \qquad (2.7)$$

ΔW is the change in weight of the cup, A is the test area, and t is the duration of the experiment, in our case 24 hr. δ is the film thickness, and ΔP (=1.333×102 Pa) is the water vapor partial pressure difference across the two sides of the film.

2.2.10 Water Solubility:

The water solubility (WS) of the films was measured, after cutting the films for 25 mm long X 25 mm width, then weighted them after drying to a constant weight at 60 °C, the small pieces were immersed in 50 ml of distilled water and kept in a Thermostatic Device Rotary Shaker (Changsha Yonglekang equipment, China) with low constant shaking (approx. 15 rpm) at RT 21 °C and RH 57% for 24 hr. After 24 hr, the films were taken from the water and dried to constant weight, to calculate the WS the following formula was used:

$$WS\ (\%) = (\Delta M/M)\times 100 \qquad (2.8)$$

where ΔM is weight loss in the water, and M is the initial weight before immersing in water respectively (Bandyopadhyay, et al., 2019).

2.2.11 Swelling ratio:

The water absorption of the hydrogel is the degree of swelling. The films were dried at room temperature until they reach the constant weight; the films were cut to 15 mm long X 15 mm wide and weighted, then all the pieces were immersed in distilled water for 330 min at room temperature, then the swollen films were wiped off with tissues paper, then weighed again. By using the following equation (Roy, et al., 2010, p.1703), the degree of swelling that corresponds to the water absorptivity of the films was calculated:

$$swelling\ ratio\% = \frac{Ws - Wd}{Wd} \times 100 \qquad (2.9)$$

Ws and Wd are weights of swollen gel and dried gel, respectively (Roy, et al., 2010, p.1703).

2.2.12 Thermal analysis:

The thermal stability of films has been tested using Thermogravimetric analysis (TGA Q500 by TA Instruments USA) based on thermal gravimetric (TG) and differential scanning calorimetry analysis (DSC). Samples were heated at 25 to 600 °C and 100 mL min^{-1} flow rate by nitrogen atmosphere at a heating rate of 10 °C min^{-1} (Bandyopadhyay, et al., 2018, p.659).

2.2.13 Biodegradability Study:

The biodegradability investigation was performed using the soil burial method in the soil combination that facilitates quicker degradation over four weeks. The samples were made by cutting them into 30 mm X 50 mm rectangular pieces and letting them on Petri dishes between the two layers of compost soil. At temperatures of 30 °C and RH 68-70 %, Petri plates were put in a humidity chamber. After wiping them using tissues that contain distilled water, the buried films were removed from the compost soil and dried up to a consistent weight each week and weighted (Bandyopadhyay, et al., 2020, p.307), (Bandyopadhyay, et al., 2019). The degradation percentage was calculated using the formula of the films in the compost:

$$D\ \% = (\Delta W/W) \times 100 \qquad (2.10)$$

D is the degradation percentage, ΔW and W are the change in weight of the films at different buried times, and the initial weight of the films, respectively (Bandyopadhyay, et al., 2020, p.307), (Bandyopadhyay, et al., 2019).

2.2.14 Drug Loading:

Cross-linked hydrogel films releasing was studied by using antibiotic clindamycin 600 mg/4ml as a model drug; the drug was incorporated into the films by using the diffusion method, where the films were immersed into a solution containing 1.8 g clindamycin in 18 ml acetone for 5 hr; after that, the films were cleaned form the residue on the surface by using distilled water, to prepare the films for releasing study.

The buffers were made by preparing three solutions, 0.2 M of KCL, 0.2 N of HCL, and 0.2 N of NaOH. All solutions were put in a volumetric flask to make a volume of 100 ml with distilled water for each one. For pH 1.4 buffer, drops of HCL solution were added to 50 ml of KCL with continuous stirring until reaching the desired pH. Also, drops of NaOH solutions were added to 50 ml KCL solution for pH 6.4 buffer.

For the calibration curve, different clindamycin concentration solutions were prepared; 2, 2.5, 3, and 4 mg/ 50 ml distilled water clindamycin concentrations were used. The UV-Vis spectrophotometer was used for the analysis of these solutions (Spectronic 601, Milton Roy, Rochester, NY, USA) (Mishra, et al., 2008, p.395).

2.2.15 Drug Release Study:

The release of entrapped drugs, clindamycin, was examined by putting the films loaded with the drug into 10 ml buffer solutions with pH 1.4 and 6.4 at 37 °C. 3 ml from the samples were periodically withdrawn every 30 min using a pipette. The sample volume was replaced with water that had been distilled. Using a UV–Vis Spectrophotometer, withdrawn quantities were examined. The maximum

absorption wavelength was determined at 150 nm. The amount of released amoxicillin was calculated using an appropriate calibration curve, curves of the released drug in pH 1.4, and 6.4 solutions were shown in Fig.7 (Mishra, et al., 2008, p.395), (Serra, et al., 2006, p.5440).

3- RESULT AND DISCUSSION.

3-1 Surface, Structural and Morphological Investigations:

The surface microscope images of the films are shown in Fig. 1, these figures clearly show the presence of holes in the surface, which, in turn, ensures the presence of pores or voids inside the films with the nature of the hydrogels.

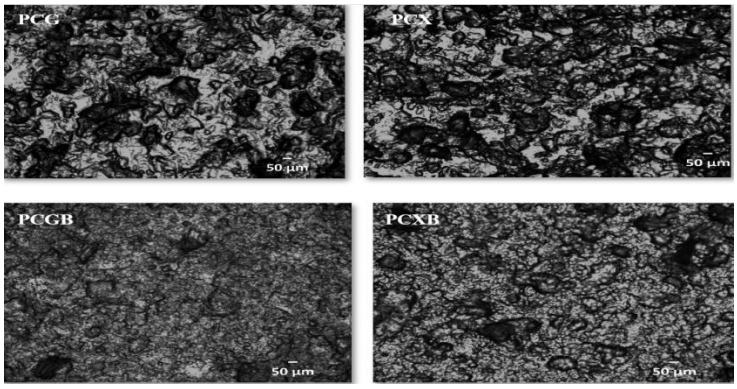

Fig. (1) Light Microscope Analysis.

In Fig. 2 where (a) the surface images and (b) cross-sectional images, the pictures show both the surface and the side parts of the film; the surface nature of the films differ, some of which directly depict the pores (Bandyopadhyay, et al., 2020, p.307), (Dai, et al., 2018, p.185) and some of which have a rough surface and even the smooth surface of the films. Some pictures show some clumps or bulges (Dai, et al., 2018, p.185). It seems that the Bentonite covers the pores on the surface as it appears in PCGB and PCXB. For cross-sectional, the images demonstrate porous presence in structure in the hydrogel (Bandyopadhyay, et al., 2020, p.307), (Bandyopadhyay, et al., 2019) despite their different sizes and shape, the pores are the gate for the exchange of gases and water vapor through the membranes, these pores appear in the form of filaments, and in some films, they appear as cracks or smaller pores accompanied with hole-shaped wrinkles. For some films, it is not easy to estimate the exact dimensions within the film and the porosity, but the general morphological information is a crucial indicator of their behaviour in water absorption and water retention capabilities (Bandyopadhyay, et al., 2018, p.659).

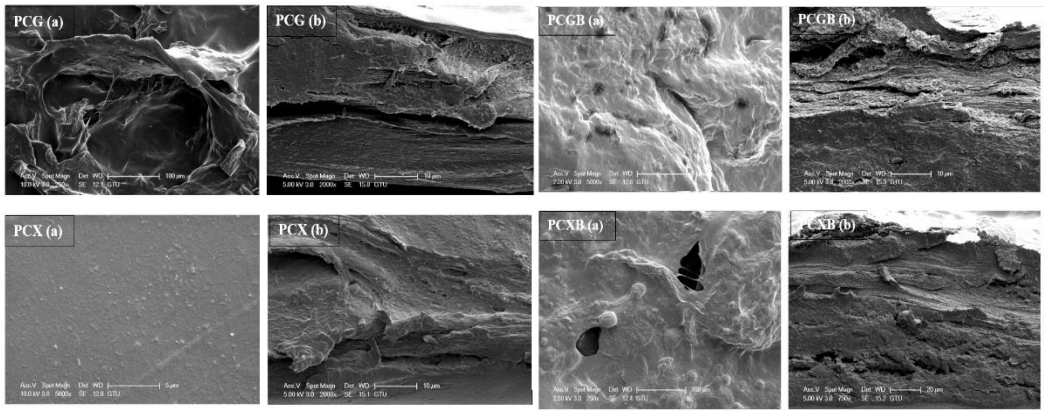

Fig. (2) SEM analysis (a) surface images and (b) cross-sectional images.

3-2 FTIR Analysis:

In Fig. 3a, FTIR is shown for the films, there are new peaks appear compared with the pure components, these peaks may refer to the presence of cross-linking bonds. In the film PCG, we can see aromatic rings, or it may be amine, NH bend, or Open-chain amino (-C=N-) at 1598 cm^{-1} and 1185 cm^{-1} Aliphatic fluoro compounds, C-F stretch, at 936 cm^{-1} Silicate ions or Primary alcohol, C-O, at 891 cm^{-1} Skeletal C-C vibrations or Vinylidene C-H out-of-plane bend. For PCGB at 887 cm^{-1} Vinylidene C-H out-of-plane bend, at 937 cm^{-1} Cyclohexane ring vibrations. For PCX at 1349 cm^{-1} Methyne C-H bend, at 933 cm^{-1} Aliphatic phosphates (P-O-C stretch), at 963 cm^{-1} trans C-H out-of-plane bend, at 739-774 cm^{-1} Aliphatic chloro compounds, C-Cl stretch. For PCXG at 3259 cm^{-1} hydrogen bond, 937-1046 cm^{-1} Cyclohexane ring vibrations, 1087 cm^{-1} Aliphatic fluoro compounds, C-F stretch (Nandiyanto, et al., 2019, p.97).

3-3 XRD Analysis:

The XRD in Fig.3b, a clear beak refers to the polymer blend showing the characteristic peaks for PVP-CMC-based polymer at 20.02°. It can be attributed to the amorphous nature of PVP for all the films, maybe it crystalline peak, and there is another peak at 16.16° for PCG film (Bandyopadhyay, et al., 2018, p.659), (Bandyopadhyay, et al., 2020, p.307) ,and (Mishra, et al., 2008, p.395)so we can notice the presence of GG in the hydrogel films may change the crystalline nature slightly and make some new peaks, and the BE can inhibit this ability.

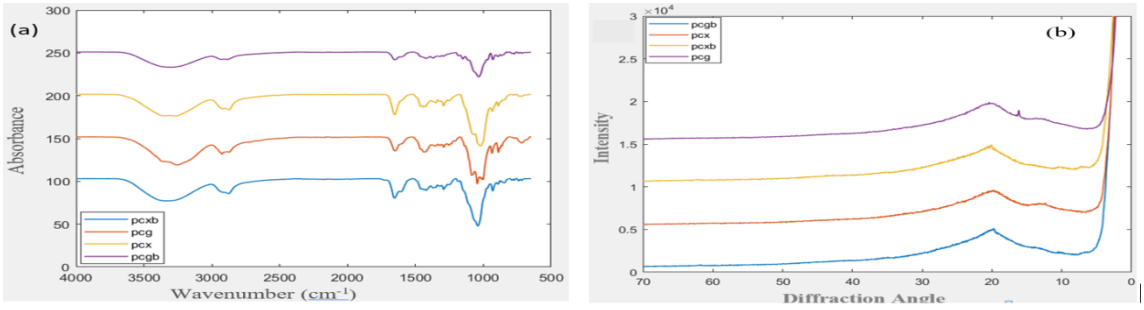

Fig. (3) (a) FTIR spectra, (b) XRD spectra.

3-4 Mechanical Properties:

The mechanical properties are important factors in biomedical fields; here, the mechanical properties are the young's modulus, elongation at break, and tensile strength (Bandyopadhyay, et al., 2010), (Bandyopadhyay, et al., 2020, p.307), (Bandyopadhyay, et al., 2019), and all are listed in Table 2; in this table, we can see the tensile strength of all the four films. We can see that young's modules or elasticity are described by the degree of deformation after the stress is removed, increase with tensile properties, and decrease elongation at break. We can refer that to the meshes of the networks (Parhi, 2017, p.515), or in other words, the differences in the polymer's arrangement and Hydrogen binding (Bandyopadhyay, et al., 2020, p.307). The best films were PCXB and PCGB, and we can refer that adding nanoparticle BE led to increasing the elasticity (Zhang, et al., 2013, p.1317); also, the presence of CMC may have attributed to the better mechanical properties, which biopolymer is expected to improve the mechanical properties of a film due to the increased affinity in the film (Bandyopadhyay, et al., 2010). Other reasons for good elasticity, may be the addition of XG enhanced the mechanical properties and incorporated with other components (da Silva Costa, et al., 2020, p.3204). Thus, PCXB and then PCGB have the best mechanical properties among the other films, so BE enhanced the mechanical properties, and the impact of the gums is clear especially XG, which makes the mechanical properties more strength.

Table (2) Tensile test of hydrogel films (E=Young's Mod, σ = tensile strength, ε= Elongation at break, F_{max}= Adhesiveness) with the standard deviation:

Hydrogel Film	E (GPa)	σ (MPa)	ε (%)	F_{max} (N)
PCG	167.93 ± 74.31	3.62 ± 1.65	10.58 ± 7.422	3.86 ±2.55
PCX	228.56 ± 94.6	3.96 ± 2.41	4.24 ± 1.55	5.68 ± 3.39
PCGB	332.98 ± 118.46	4.58 ± 1.29	3.85 ± 0.99	6.1 ± 1.72
PCXB	393.48 ± 86.54	4.23 ± 2.88	2.14 ± 1.2	6.03 ± 4.4

3-5 Colour Qualities:

The color tests are essential to determine the appearance when this film is used in biomedical soft contact lenses. In Table 3, the color test was based on standers values; we can notice that the color difference between all the films (Bandyopadhyay, et al., 2020, p.307). Thus, all the films have a slight color difference but are still visible to the human eye (Bandyopadhyay, et al., 2010), (Bandyopadhyay, et al., 2019). The chroma signifies the color purity of a material or is entangled with the brightness and emitting or reflecting surface of an object (Bandyopadhyay, et al., 2010). PCXB has the highest color difference and chroma, which means that it is darker (more yellowish) and has the minor color purity of the four films; the lightness (L), a, and b values also changed for the films with the addition of additives to the PVP-CMC base material. Here again, XG has an impact on the colours, both PCXB is darker than PCGB and PCX is darker than PCG,

and the addition of BE enhanced this ability to make the films visible, PCXB is the more visible film among the others with almost ≈ 7 in ΔE and ≈10 in C.

Table (3) Color values (L, a, and b), color differences (ΔE), Chroma (C) of the hydrogel films:

Hydrogel Film	L	a	b	ΔE	C
PCG	90.327	-0.705	6.202	3.777	5.497
PCX	89.52	-0.616	7.271	5.102	6.655
PCGB	90.213	-0.439	8.622	5.845	8.183
PCXB	89.661	-0.068	9.611	6.929	9.543

3-6 Surface Hydrophobicity:

The contact angle evaluates the surface or the material hydrophobicity, which indicates the wettability of the biofilms. In Table 4, we can observe the differences between the lower and the upper sides (Bandyopadhyay, et al., 2020, p.307); in this case, we found in the lower and upper side of the PCGB film, has lost its hydrophobicity or has low hydrophobicity compared with the other films, and for PCX, it close to being hydrophobic in the upper side, where the lower side through the experiment the water's drop did not make any contact angle, and the drop was absorbed directly. On the contrary, the contact angle of the upper and lower sides of the PCXB film was increased; It has a high hydrophobicity; it is evident that all the film's upper surface has better hydrophobicity than the lower surface (Bandyopadhyay, et al., 2019). The hydrophilic components (CMC, PEG, etc) may be compressed as they go down their tracks, in hydrogel composition (Bandyopadhyay, et al., 2020, p.307), So, the best hydrogel film is PCXB, it is evidence that BE enhanced the hydrophobicity of and XG hydrogel films, more than the other films and that's mean GG and XG films have no good surface hydrophobicity themselves, but with BE, XG's ability increased.

Table (4) The contact angle of the hydrogel films:

Hydrogel Film	Contact Angle (Θ)	
	Upper side	Lower side
PCG	101 ± 1.52	58.09 ± 1.17
PCX	85.11 ± 1.65	-
PCGB	82.19 ± 1.07	48.51 ± 1.71
PCXB	108.08 ± 1.11	72.67 ± 1.31

3-7 Permeability:

WVP test is essential for determining the barrier properties of any film; we can see from Table 5, PCGB has the best permeability while PCXB has the lowest permeability, and the reason may be for the films' permeability have decreased with the introduction of various polysaccharides to the base PVP-CMC polymeric films, The reason for the reduction in permeability may be due to the physical attractions

among phases, which made the network denser and less prone to be penetrated by the permeant. The available volume for the gaseous interchange most likely has decreased because of the reactions among different ingredients in the final polymeric network (Bandyopadhyay, et al., 2019). From this experiment, the permeability of all the films is close to each other, but the impact of adding BE on GG increased its ability while on XG decreases its ability.

Table (5) Water Vapor Permeability values of hydrogel films:

Hydrogel Film	WVP
PCG	3.52274E-07
PCX	3.79768E-07
PCGB	4.08995E-07
PCXB	3.18001E-07

3-8 Solubility Assay:

The ability to be dissolved, especially in water, is known as solubility, in **Fig. 4a**; the results of the solubility test are shown, The PCG film is less solubility, and that may be because of the strong hydrogen bond that is produced (Bandyopadhyay, et al., 2019), compared with all the films, PCXB film has more solubility than the rest. Both bentonite films were significantly soluble in water, compared with the PCXB film which was soluble more than the other films. However, despite GG and XG having high solubility in general (Kadajji & Betageri, 2011, p.1972), the effect of BE was remarkable for both. Both BE films were significantly soluble in water. Furthermore, PCXB underwent structural deformation. In contrast, the other films kept their shapes during the solubility assay. We can notice that GG solubility is less than XG in both cases, and no changes in the order with BE, which means XG is good soluble itself, and with BE this ability increased.

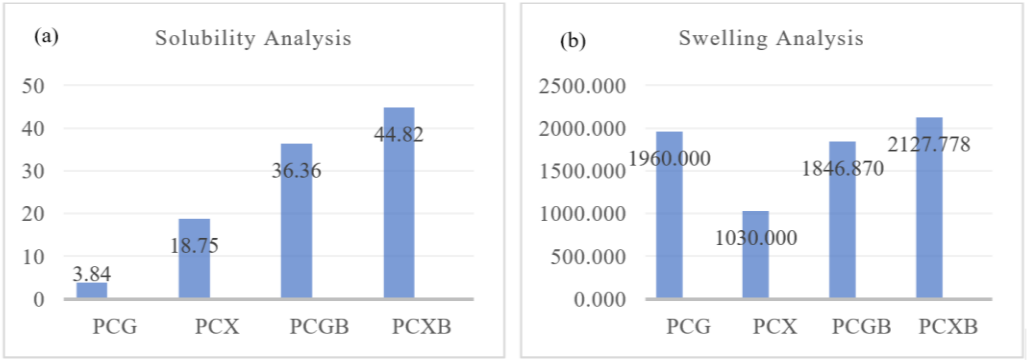

Fig. (4) (a) Solubility analysis, (b) Swelling Analysis.

3-9 Swelling Assay:

Hydrogel swelling is typically defined as an accumulation of fluid, in Fig. 4b, the films show good swelling properties, add to that GG and XG are soluble themselves (Kadajji & Betageri, 2011, p.1972). The best

film is PCXB, although PCXB is highly soluble, it has a high swelling behavior also; To understand this, we should know the thermodynamic and kinetics factors determined by the time, so changes in the cross-linking make the polymer soluble and swollen, and layer thickness decreases with time due to the desorption of polymer chains (Miller-Chou, et al., 2003, p.1223), (Tempelman, 2019). Thus, the best-swollen film is PCXB. Furthermore, PCGB with PCXB, both contain BE. It was mentioned in (Dai, et al., 2018, p.185) that BE increases the swelling abilities, especially with XG.

3-10 Thermal Analysis:

The thermal behavior of films was studied in Fig. 5, based on the carves on figures, we investigate the degradation of the hydrogel films almost divided into three stages (Gils, et al., 2009, p.364), (Dai, et al., 2018, p.185), the first stages are below 110 °C for PCGB, and below 100 °C for PCXB, PCG, and PCX, which small weight is lost from all the films, but guar gums films lost it more. They may be due to the water evaporation from the films. The second stage in all the films was the significant weight loss from 150 to 320 °C for PCG, 150 to 340 °C for PCX, and PCGB, for PCXB 90 to 380 °C. The final further weight loss beyond 350 to 480 °C for PCG, 360 to 460 °C for PCX, for PCGB 370 to 500 °C, and PCXB 410 °C to 490 °C have corresponded to the decomposition of oxygen-containing groups like hydroxyl, carboxyl, and/or epoxide groups, The decomposition process finish at around 500 °C with almost80% weight loss for all the films (Bandyopadhyay, et al., 2020, p.307). We can notice that PCGB and PCXB were the last degraded films, so based on the results, the addition of BE could enhance the thermal stability of hydrogel films (Dai, et al., 2018, p.185). Thus, PCGB and PCXB films both have excellent thermal stability, and if the films contain no BE, still GG film is better than XG.

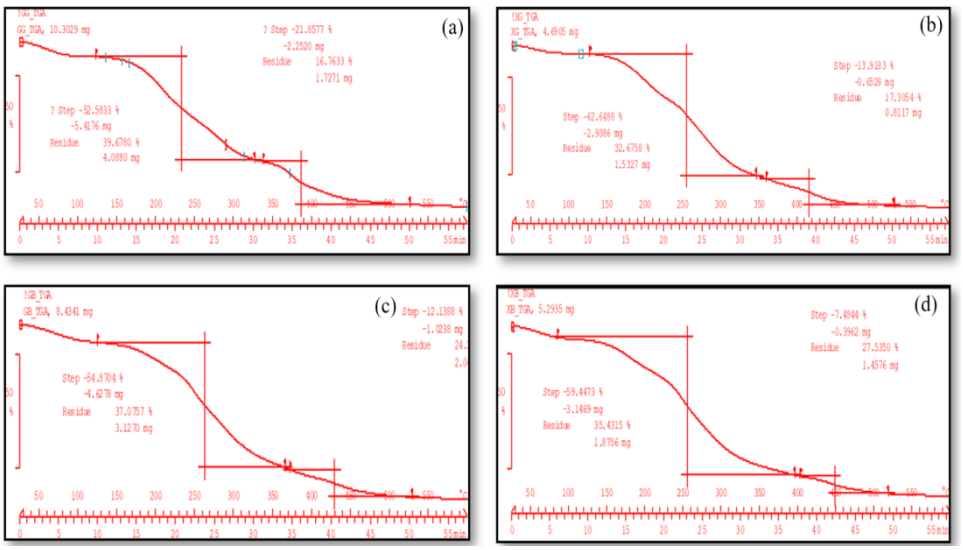

Fig. (5) Thermal analysis (a) PCG Film (b) PCX film (d) PCGB film (d) PCXB films.

3-11 Biodegradability Study:

The significance of hydrogel is strongly influenced by biodegradation study. It is one of the most important aspects that explain the impact of these films on the environment, as well as the potential of their being converted into harmless material, particularly in soil. The findings of this experiment are given in Table 6, which depicts the deterioration of the films over four weeks and their initial weight. All of the hydrogel films demonstrated their remarkable ability to biodegrade even in the absence of earthworms and only by the action of compost-rich soil during the trial period, as the films disintegrated and lost more than three-quarters of their weight (30 days). BE has little influence on decomposition rates, as evidenced by the fact that films containing BE and those without it disintegrate at nearly the same rates, while the addition of GG has an impact.

One of the other findings of this study is that most of the films turned brown and did not return to their original color even after being washed with distilled water, indicating that soil content penetration and spread of soil moisture through the films continue and that the degradation continues. Film thickness has also decreased dramatically every week. What evidence do you have that the film has lost weight? This research backs up previous findings on the degradation of hydrogel films, which showed that breaking glycosidic bonds in the polymer chains leaves behind other free-moving components like PEG, which degrade slowly, and PVP, which may remain in the soil without causing any negative environmental effects.

These films might decay to 90-95 % of their original weight if the burry time is extended for another three weeks. So, PCG and PCGB are the most degraded films, which means GG itself is the factor in increasing biodegradation.

Table. (6) Biodegradation of the films and the initial weight.

Hydrogel Film	Initial weight (g)	weight (week 1)	weight (week 2)	weight (week 3)	weight (week 4)	D%
PCG	0.097	0.082	0.066	0.051	0.036	62.886
PCX	0.111	0.094	0.078	0.061	0.049	55.855
PCGB	0.148	0.126	0.103	0.081	0.058	60.810
PCXB	0.121	0.108	0.093	0.079	0.064	47.107

3-12 Releasing Study:

The amount of drug release from hydrogel films was evaluated in this study. The release of water-soluble medicines trapped in hydrogels occurs when water enters the polymer network to expand and dissolve the drug. This medication diffuses to the film surface via the waterways. As illustrated in Fig. 6, a clindamycin release profile for drug-loaded hydrogel films was provided in various liberation media or buffers, pH 1.4 and pH 6.4.

All of the films have demonstrated a high level of drug release. It can also be seen that all films release the drug in the same manner. In a film PCGB, the maximum drug release rate was reported at 33% after 30 minutes When the medium was pH 1.4, the lowest rate of release was 31% in a film PCX. Following that, the films returned to release in a bigger number, surpassing 43 % of the film PCX and around 40 % of the film PCG after 90 minutes, before gradually decreasing.

When the medium was pH 6.4, the films reacted similarly, with the maximum release reported at around 33% for a film PCX and 31% for a film PCXB at the 30th minute. After that, during the 90th minute, the film's releases a significant quantity of over 45 % for a PCGB film and above 40 % for PCG, and then the release rate drops somewhat.

According to this method, around 95-99 % of the medication will be released from the films after about 5 hours, ensuring the films' efficiency in loading and discharging medicines. We may infer that the film PCGB containing BE had the best release when tested at a medium pH of 6.4, whereas the PCXB film had the highest release when tested at a medium pH of 1.4. Even though the percentages are almost similar, the drug release at medium pH 6.4 was significantly higher. So, we can understand the impact of adding BE in the releasing properties of the drug in the hydrogel films, and that is clear in PCGB and PCXB films, and that could be noticed separately in GG films which have low releasing abilities.

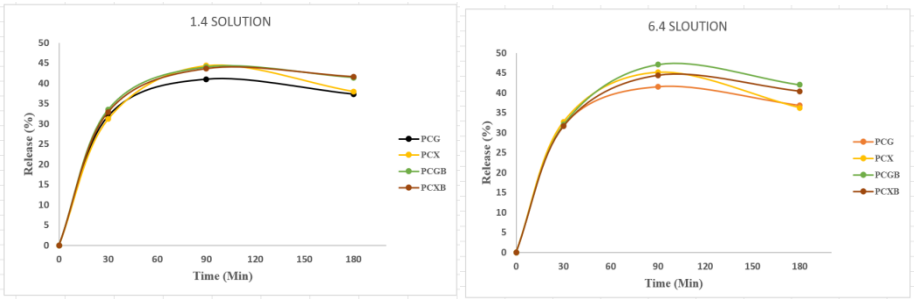

Figure. (6) (a) released drug in 1.4 pH solution, and (b) released drug in 6.4 pH solution.

4- CONCLUSION.

In this study, four PVP-CMC- gums based on hydrogel films were produced, and the impact of adding Gums, and Bentonite clay were studied; all the results show that Bentonite enhanced most of the properties of hydrogel films, and we can refer that sometimes to the addition of the gum which means these films can be used in various biomedical applications based on the main desired feature of the application.

From the results, we can see the new peaks of the film, which are different from the pure materials, and that means, in these films, some reactions and bindings happened and played a role in creating new cross-linking, which ensures the high success of these hydrogel films in specific biomedical applications such as drug delivery. SEM and Microscope showed the possibility of founding porous structure inside the films, we can conclude from color, surface hydrophobicity, solubility, and swelling,

properties PCXB film is the best. In contrast, PCGB film has the best results in biodegradation and permeability results, and both have excellent thermal stability, mechanical properties, and releasing behaviors. Consequently, the prepared hydrogels, especially PCGB and PCXB, can be applied in different biomedical applications.

REFERENCES.

[1] Gils, P. S., Ray, D., & Sahoo, P. K. (2009). "*Characteristics of xanthan gum-based biodegradable super porous hydrogel*". International journal of biological macromolecules, 45(4), 364-371.

[2] Ma, J., Li, X., & Bao, Y. (2015). "*Advances in cellulose-based superabsorbent hydrogels*". RSC advances, *5*(73), 59745-59757.

[3] Ahmed, E. M. (2015). "*Hydrogel: Preparation, characterization, and applications: A review*". Journal of advanced research, 6(2), 105-121.

[4] Roy, N., Saha, N., Kitano, T., & Saha, P. (2010). "*Novel hydrogels of PVP–CMC and their swelling effect on viscoelastic properties*". Journal of Applied Polymer Science, 117(3), 1703-1710.

[5] Roy, N., Saha, N., Kitano, T., & Saha, P. (2010). "*Development and characterization of novel medicated hydrogels for wound dressing*". Soft Materials, 8(2), 130-148. (Ray, et al., 2010, p.130)

[6] Bandyopadhyay, S., Saha, N., Brodnjak, U. V., & Saha, P. (2018). "*Bacterial cellulose based greener packaging material: A bioadhesive polymeric film*". Materials Research Express, 5(11), 115405.

[7] Bandyopadhyay, S., Saha, N., Zandraa, O., Pummerová, M., & Sáha, P. (2020). "*Essential oil based PVP-CMC-BC-GG functional hydrogel sachet for 'cheese': its shelf life confirmed with anthocyanin (Isolated from red cabbage) bio stickers*". Foods, 9(3), 307.

[8] Haaf, F., Sanner, A., & Straub, F. (1985). "*Polymers of N-vinylpyrrolidone: synthesis, characterization and uses*". Polymer Journal, 17(1), 143-152.

[9] Hsiao, C. N., & Huang, K. S. (2005). "*Synthesis, characterization, and applications of polyvinylpyrrolidone/SiO2 hybrid materials*". Journal of applied polymer science, 96(5), 1936-1942.

[10] Batelaan, J. G., Van Ginkel, C. G., & Balk, F. (1992). "*Carboxymethylcellulose (cmc)*". Detergents, Springer, Berlin, Heidelberg, 329-336.

[11] Kanikireddy, V., Varaprasad, K., Jayaramudu, T., Karthikeyan, C., & Sadiku, R. (2020). "*Carboxymethyl cellulose-based materials for infection control and wound healing: A review*". International Journal of Biological Macromolecules, 164, 963-975.

[12] Armisen, R., & Galatas, F. (1987). "*Production, properties and uses of agar. Production and utilization of products from commercial seaweeds*". Fao Fisheries Technical, 288, 1-57.

[13] Hutanu, D., Frishberg, M. D., Guo, L., & Darie, C. C. (2014). "*Recent applications of polyethylene glycols (PEGs) and PEG derivatives*". Modern Chemistry and Applications, 2(2), 1-6.

[14] Bandyopadhyay, S., Saha, N., Brodnjak, U. V., & Sáha, P. (2019). "*Bacterial cellulose and guar gum based modified PVP-CMC hydrogel films: Characterized for packaging fresh berries*". Food Packaging and Shelf Life, 22, 100402.

[15] Mudgil, D., Barak, S., & Khatkar, B. S. (2014). "*Guar gum: processing, properties and food applications—a review".* Journal of food science and technology, 51(3), 409-418.

[16] Garcıa-Ochoa, F., Santos, V. E., Casas, J. A., & Gómez, E. (2000). "*Xanthan gum: production, recovery, and properties".* Biotechnology advances, 18(7), 549-579.

[17] Adamis, Z., Williams, R. B., & Fodor, J. (2005). Bentonite, kaolin, and selected clay minerals (No. 231). World Health Organization.

[18] Stojiljković, S. T., & Stojiljković, M. S. (2017). "*Application of Bentonite Clay for Human Use".* In Proceedings of the IV Advanced Ceramics and Applications Conference, 349-356.

[19] Roy, N., Saha, N., Kitano, T., & Saha, P. (2010). "*Novel hydrogels of PVP–CMC and their swelling effect on viscoelastic properties*". Journal of Applied Polymer Science, 117(3), 1703-1710.

[20] Bandyopadhyay, S., Saha, N., & Sáha, P. (2018). "*Characterization of bacterial cellulose produced using media containing waste apple juice*". Applied Biochemistry and Microbiology, 54(6), 649-657.

[21] Dai, H., Huang, Y., & Huang, H. (2018). "*Eco-friendly polyvinyl alcohol/carboxymethyl cellulose hydrogels reinforced with graphene oxide and bentonite for enhanced adsorption of methylene blue*". Carbohydrate polymers, 185, 1-11.

[22] Nandiyanto, A. B. D., Oktiani, R., & Ragadhita, R. (2019). "*How to read and interpret FTIR spectroscope of organic material*". Indonesian Journal of Science and Technology, 4(1), 97-118.

[23] Mishra, R. K., Datt, M., & Banthia, A. K. (2008). "*Synthesis and characterization of pectin/PVP hydrogel membranes for drug delivery system*". Aaps Pharmscitech, 9(2), 395-403.

[24] Serra L., Doménech J., & Peppas N. A., (2006), "*Drug transport mechanisms and release kinetics from molecularly designed poly (acrylic acid-g-ethylene glycol) hydrogels*", Journal of Biomaterials, 27 (31), 5440-5451.

[25] Parhi, R. (2017). "*Cross-linked hydrogel for pharmaceutical applications: a review*". Advanced pharmaceutical bulletin, 7(4), 515-530.

[26] Zhang, P., Guan, Q., & Li, Q. (2013). Mechanical properties of plastic concrete containing bentonite. *Research Journal of Applied Sciences, Engineering and Technology*, *5*(4), 1317-1322.

[27] da Silva Costa, R. A., Bonomo, R. C. F., Rodrigues, L. B., Santos, L. S., & Veloso, C. M. (2020). "*Improvement of texture properties and syneresis of arrowroot (Maranta arundinacea) starch gels by using hydrocolloids (guar gum and xanthan gum)*". Journal of the science of food and agriculture, 100(7), 3204-3211.

[28] Kadajji, V. G., & Betageri, G. V. (2011). "*Water soluble polymers for pharmaceutical applications*". Polymers, 3(4), 1972-2009.

[29] Miller-Chou, B. A., & Koenig, J. L. (2003). "*A review of polymer dissolution*". Progress in Polymer Science, 28(8), 1223-1270.

[30] Tempelman, K. (2019). Swelling of thin polymer films: understanding the mechanisms and dynamics. University of Twente.